Neuropsychopharmacology (2015), 1–10

www.neuropsychopharmacology.org

Neural Correlates of Three Promising Endophenotypes of Depression: Evidence from the EMBARC Study

Christian A Webb[1], Daniel G Dillon[1], Pia Pechtel[1], Franziska K Goer[1], Laura Murray[1], Quentin JM Huys[2,3], Maurizio Fava[4], Patrick J McGrath[5], Myrna Weissman[5], Ramin Parsey[6], Benji T Kurian[7], Phillip Adams[5], Sarah Weyandt[7], Joseph M Trombello[7], Bruce Grannemann[7], Crystal M Cooper[7], Patricia Deldin[8], Craig Tenke[5], Madhukar Trivedi[7], Gerard Bruder[5] and Diego A Pizzagalli*[,1]

[1]Department of Psychiatry, Harvard Medical School and McLean Hospital, Belmont, MA, USA; [2]Centre for Addiction Disorders, Department of Psychiatry, Psychotherapy and Psychosomatics, Hospital of Psychiatry, University of Zurich, Switzerland; [3]Translational Neuromodeling Unit, Institute for Biomedical Engineering, University of Zurich and Swiss Federal Institute of Technology (ETH) Zurich, Switzerland; [4]Clinical Research Program, Massachusetts General Hospital, Boston, MA, USA; [5]Department of Psychiatry, New York State Psychiatric Institute, College of Physicians and Surgeons of Columbia University, New York, NY, USA; [6]Department of Psychiatry and Behavioral Science, Stony Brook University, Stony Brook, NY, USA; [7]Department of Psychiatry, University of Texas Southwestern Medical Center, Dallas, TX, USA; [8]Department of Psychiatry, University of Michigan Health System, Ann Arbor, MI, USA

Major depressive disorder (MDD) is clinically, and likely pathophysiologically, heterogeneous. A potentially fruitful approach to parsing this heterogeneity is to focus on promising endophenotypes. Guided by the NIMH Research Domain Criteria initiative, we used source localization of scalp-recorded EEG resting data to examine the neural correlates of three emerging endophenotypes of depression: neuroticism, blunted reward learning, and cognitive control deficits. Data were drawn from the ongoing multi-site EMBARC study. We estimated intracranial current density for standard EEG frequency bands in 82 unmedicated adults with MDD, using Low-Resolution Brain Electromagnetic Tomography. Region-of-interest and whole-brain analyses tested associations between resting state EEG current density and endophenotypes of interest. Neuroticism was associated with increased resting gamma (36.5–44 Hz) current density in the ventral (subgenual) anterior cingulate cortex (ACC) and orbitofrontal cortex (OFC). In contrast, reduced cognitive control correlated with decreased gamma activity in the left dorsolateral prefrontal cortex (dlPFC), decreased theta (6.5–8 Hz) and alpha2 (10.5–12 Hz) activity in the dorsal ACC, and increased alpha2 activity in the right dlPFC. Finally, blunted reward learning correlated with lower OFC and left dlPFC gamma activity. Computational modeling of trial-by-trial reinforcement learning further indicated that lower OFC gamma activity was linked to reduced reward sensitivity. Three putative endophenotypes of depression were found to have partially dissociable resting intracranial EEG correlates, reflecting different underlying neural dysfunctions. Overall, these findings highlight the need to parse the heterogeneity of MDD by focusing on promising endophenotypes linked to specific pathophysiological abnormalities.

Neuropsychopharmacology advance online publication, 1 July 2015; doi:10.1038/npp.2015.165

INTRODUCTION

Major depressive disorder (MDD), as currently defined, represents a highly heterogeneous disorder that is etiologically and pathophysiologically complex. One potentially promising approach to parsing this heterogeneity is the investigation of endophenotypes (Chan and Gottesman, 2008; Gottesman and Gould, 2003). Endophenotypes are assumed to lie on the pathway between genotype and disease, and be less complex than the downstream symptom clusters that currently define psychiatric diagnoses. Gottesman and colleagues proposed that endophenotypes must meet the following criteria: (1) be associated with the disease; (2) be heritable; (3) be primarily state-independent; (4) cosegregate within families; (5) be more common in non-affected family members of individuals with the disease compared with the general population; and (6) be measured reliably.

Neuroticism, blunted reward learning and cognitive control deficits have emerged as among the most promising behavioral endophenotypes of depression (Goldstein and Klein, 2014; Pizzagalli, 2014; Snyder, 2013), and map well onto central Research Domain Criteria (RDoC) domains, particularly negative valence systems (neuroticism), positive valence systems (reward learning), and cognitive systems (cognitive control). First, neuroticism—the propensity to experience negative emotions—is elevated in current and remitted depression (De Fruyt *et al*, 2006; Klein *et al*, 2011), and predicts first onset of MDD (Kendler *et al*, 2006). Twin

*Correspondence: Dr DA Pizzagalli, Center for Depression, Anxiety, and Stress Research, McLean Hospital, Harvard Medical School, 115 Mill Street, Belmont, MA 02478, USA, Tel: +1 617 855 4230, Fax: +1 617 855 4230, E-mail: dap@mclean.harvard.edu
Received 16 February 2015; revised 24 April 2015; accepted 27 May 2015; accepted article preview online 12 June 2015

studies indicate that neuroticism shares significant genetic variance with depression, and is moderately heritable (eg, Birley *et al*, 2006; Kendler *et al*, 2006). Moreover, neuroticism cosegregates within families (Farmer *et al*, 2002; Ouimette *et al*, 1996), and non-depressed family members of those with MDD have higher levels of neuroticism than the general population (Modell *et al*, 2003). Finally, measures of neuroticism (eg, NEO Personality Inventory) have relatively strong psychometric properties (Costa *et al*, 2005).

Second, blunted reward learning—defined as a diminished ability to modulate behavior as a function of rewards—has been observed in both individuals with current and remitted MDD (Goldstein and Klein, 2014; Pechtel *et al*, 2013; Pizzagalli, 2014). A twin study estimated the heritability of reward learning to be 0.46 (Bogdan and Pizzagalli, 2009), as assessed by a commonly used Probabilistic Reward Task (PRT; Pizzagalli *et al*, 2005a). In addition, the same study reported a moderate ($r = 0.29$) genetic correlation between depression and reward learning. Data related to the reliability of reward learning is limited, with one study finding significant test–retest reliability ($r = 0.57$) over 38 days (Pizzagalli *et al*, 2005a). To our knowledge, no study has evaluated whether reward learning fulfills the cosegregation or familial association endophenotype criteria.

Finally, MDD is characterized by broad impairments in cognitive control, which often persist following remission (Snyder, 2013) and exhibit trait-like stability (Sarapas *et al*, 2012). Moderate-to-high heritability (Friedman *et al*, 2008; Stins *et al*, 2004), as well as strong test–retest reliability and internal consistency (Wöstmann *et al*, 2013) have been reported for commonly used cognitive control paradigms (eg, Stroop, Eriksen Flanker). In addition, there is evidence of cognitive control impairments in healthy, unaffected twins discordant for MDD (Christensen *et al*, 2006). Evidence for cosegregation and familial association is lacking.

With regards to neural substrates, neuroticism has been associated with increased amygdala and anterior cingulate cortex (ACC) activity (Haas *et al*, 2007; Servaas *et al*, 2013), both in the 'affective' (ie, rostral (rACC) and subgenual (sgACC)) and 'cognitive' subdivisions (ie, dorsal (dACC)). In contrast, tasks tapping reward learning have been shown to recruit the striatum, orbitofrontal cortex (OFC; Hornak *et al*, 2004; O'Doherty, 2004), dACC (Rushworth *et al*, 2007; Santesso *et al*, 2008), and left dorsolateral prefrontal cortex (dlPFC; BA 9/46; Ahn *et al*, 2013; Pizzagalli *et al*, 2005b), especially in tasks requiring integration of reinforcements over time (eg, PRT). Finally, cognitive control has been reliably linked to the dlPFC and dACC (Pizzagalli, 2011; Ridderinkhof *et al*, 2004).

Inspired by the RDoC initiative, the goal of this study was to examine the association between these three candidate endophenotypes and intracranial estimates of resting brain electrical activity (EEG) in an unmedicated depressed sample. We employed a region-of-interest (ROI) approach, followed by an exploratory whole-brain analysis to test the specificity of ROI findings. ROIs were selected based on the literature reviewed above, and within the constraints of EEG source localization techniques, which cannot probe subcortical structures (eg, amygdala, caudate). Based on prior studies, we hypothesized that: (1) neuroticism would be associated with greater resting activity in the affective (rACC/sgACC) and cognitive (dACC) subdivisions of the ACC; (2) blunted reward learning would be linked to lower activity in the OFC, dACC, and left dlPFC; and (3) reduced cognitive control would correlate with lower activity in the dlPFC and cognitive (dACC)—but not affective—ACC subdivision. Finally, a cluster analysis was conducted in an effort to empirically derive subgroups of depressed patients on the basis of endophenotype profiles.

MATERIALS AND METHODS

Data were collected in a multi-site clinical trial entitled 'Establishing Moderators and Biosignatures of Antidepressant Response for Clinical Care for Depression' (EMBARC). Recruiting sites are Columbia University (CU), Massachusetts General Hospital (MGH), the University of Texas Southwestern Medical Center (UT), and the University of Michigan (UM). Participants completed several behavioral, self-report, and physiological assessments before enrolling in the double-blind, placebo-controlled clinical trial of sertraline and bupropion. Data collection for the treatment phase is ongoing and the blind remains unbroken. Accordingly, the current study only considers baseline resting EEG, behavioral (Flanker and PRT), and self-report (NEO) data for the first 100 MDD subjects. Participants provided informed consent following procedures approved by site IRBs.

Participants

Eligible participants (aged 18–65 years) met DSM-IV criteria for a current MDD episode (SCID-I/P), scored 14 or above on the 16-item Quick Inventory of Depression Symptomatology (Rush *et al*, 2003), and were medication free for >3 weeks before completing any study measures. Exclusion criteria included: history of psychosis or bipolar disorder; substance dependence in the past 6 months (excluding nicotine) or substance abuse in the past 2 months; active suicidality; or unstable medical conditions (for more information about the sample, see Supplementary Materials). Data from 82 MDD subjects who passed quality control criteria for both Flanker and PRT (see Supplementary Materials) and had NEO scores were analyzed.

Measures

NEO Five-Factor Inventory: 3 (NEO-FFI-3). The NEO-FFI is a 60-item self-report questionnaire assessing Neuroticism, Extraversion, Openness, Agreeableness and Conscientiousness (12 items/factor; McCrae and Costa, 2010).

Probabilistic Reward Task (PRT). The PRT uses a differential reinforcement schedule to probe reward learning (ie, the ability to modulate behavior as a function of rewards), and has been described in detail (Pizzagalli *et al*, 2005a, 2008; see Supplementary Materials). Participants performed two blocks of 100 trials.

Flanker Task. A modified version of the Eriksen Flanker Task with an individually titrated response window was used (Eriksen and Eriksen, 1974; Holmes *et al*, 2010). Participants first completed a practice session followed by five blocks consisting of 70 trials each (46 congruent and 24 incongruent), for a total of 350 trials. On each trial, participants

pressed a button to indicate whether a center arrow pointed left or right. The central arrow was presented with adjacent flankers, which either pointed in the same direction (congruent condition) or the opposite direction (incongruent condition) as the central arrow (see Supplementary Materials). Both accuracy and reaction time (RT) were recorded.

Hamilton Rating Scale for Depression (HRSD). The 32-item HRSD is a clinician-administered measure of depressive symptom severity (Hamilton, 1960). It was administered by trained clinical evaluators.

Data Acquisition and Reduction

Resting EEG recording consisted of four contiguous 2-min trials (two eyes open, two eyes closed), for a total of 8 min. Site certification, intersite standardization, quality assurance, and preprocessing of resting EEG for all sites were performed at the Columbia site (see Supplementary Materials for details). McLean Hospital was responsible for site training and certification, quality assurance, and analysis of Flanker and PRT data as well as Low-Resolution Brain Electromagnetic Tomography (LORETA) analyses. Hypotheses were tested for the theta (6.5–8 Hz), alpha1 (8.5–10 Hz), alpha2 (10.5–12 Hz), and gamma (36.5–44 Hz) frequency bands (for rationale, see Supplementary Materials). LORETA (Pascual-Marqui *et al*, 1999) was used to estimate the three-dimensional intracerebral current density distribution for each frequency band. With respect to the ACC, to test the specificity of findings, LORETA voxels corresponding to the affective (BA25 (sgACC); BA24/32 (rACC)) and cognitive (BA24'/32' (dACC)) subdivisions were identified (Pizzagalli, 2011). Similarly, anatomical considerations were used to identify the dlPFC (lateral BA9 and BA46) and OFC (BA11/13/47/12; Kringelbach and Rolls, 2004; see Supplementary Material, Supplementary Figure 1, for ROI definitions). For each ROI, intensity-normalized current density was averaged across voxels.

Probabilistic Reward Task. The primary variable of interest was change in *response bias* (RB) scores from the first to the second block ($RB_{Block2} - RB_{Block1}$), which reflects reward learning. In addition, *discriminability* scores, indexing the ability to differentiate between stimuli, were included as a covariate in specificity analyses (for formulas, see Supplementary Materials). The development of a RB depends both on the sensitivity to individual rewarding feedback and the ability to incrementally associate stimuli/actions with rewards over the course of the task. To discriminate between these components of reward learning, we fitted a series of reinforcement learning models to trial-by-trial behavioral data as described previously (Huys *et al*, 2013). These contained two key parameters: *reward sensitivity*, which indexes the reinforcing strength of the individual reward outcomes, and *learning rate*, which measures the ability to progressively associate outcomes with antecedent stimuli/actions (see Supplementary Materials).

Flanker task. The primary variables of interest were the *interference effects*: lower accuracy and longer RTs on incongruent than congruent trials. These effects were computed as ($Accuracy_{Compatible\ trials} - Accuracy_{Incompatible\ trials}$) and ($RT_{Incompatible\ trials} - RT_{Compatible\ trials}$).

Statistical Analyses

For ROI-based analyses, four separate sets of multiple regressions were run to examine the association between LORETA-derived EEG current density and (1) neuroticism, (2) reward learning, and the Flanker interference effects on both (3) accuracy and (4) RT. For neuroticism, current density in the affective (sgACC and rACC) and cognitive (dACC) subdivisions of the ACC were entered as predictors. For reward learning, current density in the OFC, left and right dlFPC, and dACC were entered as predictors. Finally, for Flanker interference effects, separate multiple regressions were run for accuracy and RT, with current density in the rACC, dACC, and left/right dlPFC serving as predictors. Regressions were run separately for each frequency band. All predictor variables were entered simultaneously in multiple regression models, and all models included site (CU/MGH/UT/UM) as a covariate. For significant findings, specificity analyses were performed to test whether associations remained when accounting for (1) depression severity (by entering HRSD scores as an additional predictor) and (2) the other endophenotypes. In addition, to the extent that significant findings emerged in the reward learning analyses, we followed-up with two multiple regressions testing whether significant ROIs also predicted the *reward sensitivity* and *learning rate* parameters extracted from the computational models. Regression analyses were carried out using SAS version 9.2 PROC GLM. [Several univariate outliers (absolute value $z > 3.0$) were identified. Specifically, gamma, theta, alpha1, and alpha2 current density values in BA24/32 (rACC) for 1 subject; theta, alpha1 and alpha2 in BA24'/32' (dACC) for 1 subject; gamma and alpha1 left dlPFC values for 1 subject. These data were omitted from the relevant analyses.]

To evaluate regional specificity, exploratory whole-brain correlational analyses were conducted between (1) neuroticism, reward learning and Flanker interference effects, and (2) current density in the theta, alpha1, alpha2, and gamma bands separately. To control for multiple comparisons, analyses were carried out using the 'Randomise' permutation-based inference tool in FSL for nonparametric statistical thresholding (5000 permutations, $p < 0.05$, FWE corrected; Winkler *et al*, 2014). Finally, in an effort to empirically derive subgroups of depressed patients on the basis of endophenotype measures, a two-step cluster analysis was conducted in SPSS (Version 20) using the Log-likelihood distance measure and Schwarz's Bayesian Information Criterion as clustering criteria (Chiu *et al*, 2001; Fava *et al*, 2012), and without prespecifying the desired number of clusters.

RESULTS

Supplementary Table 1 provides a summary of significant ROI findings.

Neuroticism

The first regression predicted neuroticism scores, with gamma current density in the cognitive (dACC) and affective (sgACC) ACC subdivisions entered as predictors. As

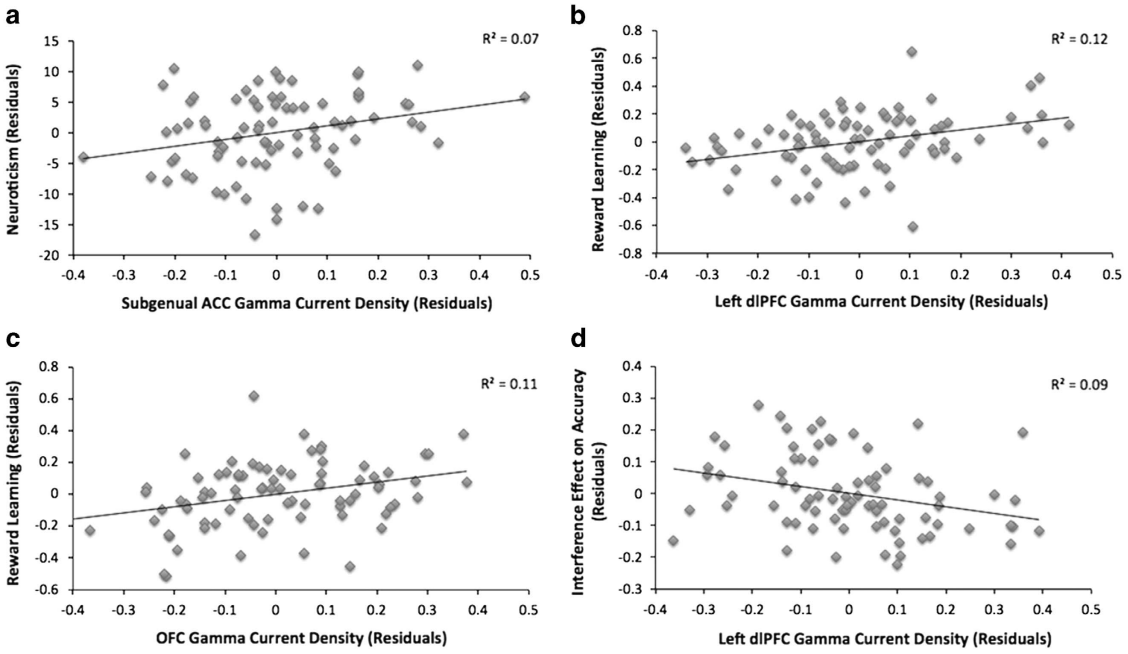

Figure 1 Partial regression plots displaying the association between (a) neuroticism and gamma current density in the subgenual anterior cingulate cortex (sgACC; BA25), after controlling for the model covariates (site and gamma activity in BA 24'/32' (dACC)); (b) reward learning and gamma activity in the left dorsolateral prefrontal cortex (dlPFC), after controlling for the model covariates (site and gamma activity in the right dlPFC, dACC, and orbitofrontal cortex (OFC)); (c) reward learning and gamma activity in the OFC, after controlling for the model covariates (site and gamma activity in the left and right dlPFC, and dACC); (d) Flanker interference effect on accuracy and gamma activity in the left dlPFC, after controlling for the model covariates (site and gamma activity in the right dlPFC, dACC, and BA 24/32 (rACC)). The association in panel a remains significant ($\beta = 0.29$, $p = 0.030$) after removing the sgACC residual value at the far right of panel.

expected, when controlling for dACC, gamma activity in sgACC was associated with neuroticism ($\beta = 0.31$, $p = 0.018$; Figure 1a). In contrast, gamma activity in dACC did not predict neuroticism ($\beta = -0.01$, $p = 0.965$). An analogous model entering gamma current density in the dACC and rACC yielded a nonsignificant trend between rACC and neuroticism ($\beta = 0.24$, $p = 0.054$; dACC: $\beta = -0.07$, $p = 0.646$). [Given the very high correlation between current density in BA25 (sgACC) and neighboring BA24/32 (rACC) (for gamma, $r = 0.74$), these variables were included as predictors in separate regression models to minimize multicollinearity.] No significant predictors emerged for the theta or alpha bands (p's > 0.15).

Specificity analyses. The relationship between sgACC gamma activity and neuroticism remained when accounting for (1) current depressive symptoms (HRSD) and the other NEO personality factors ($\beta = 0.27$, $p = 0.024$); and (2) Flanker interference effects and reward learning ($\beta = 0.29$, $p = 0.025$).

Reward Learning

Greater gamma activity in the OFC ($\beta = 0.33$, $p = 0.004$) and left dlPFC ($\beta = 0.34$, $p = 0.002$)—but not right dlPFC ($\beta = -0.11$, $p = 0.358$) or dACC ($\beta = -0.05$, $p = 0.682$)—predicted reward learning (Figure 1b and c). Importantly, the correlations between reward learning and gamma activity in the left ($r = 0.31$, $p = 0.005$) and right dlPFC ($r = -0.04$, $p = 0.711$) were significantly different ($z = 2.36$, $p = 0.018$; Meng *et al*, 1992). Models considering theta and alpha current density yielded no significant associations (p's > 0.06).

Specificity analysis. The relationships between gamma activity in the OFC/left dlPFC and reward learning remained significant when accounting for (1) current depressive symptoms and PRT discriminability (both β's $= 0.34$, $p < 0.005$); and (2) neuroticism and the Flanker interference effects (OFC: $\beta = 0.33$, $p = 0.008$; left dlPFC: $\beta = 0.41$, $p < 0.001$).

Computational modeling. A multiple regression indicated that gamma activity in the OFC ($\beta = 0.27$, $p = 0.043$)—but not the left dlPFC ($\beta = 0.11$, $p = 0.378$)—positively predicted reward sensitivity. No significant findings emerged in the prediction of learning rate (p's > 0.20).

Cognitive Control

Flanker interference effect (accuracy). The regression revealed that gamma activity in the left dlPFC ($\beta = -0.31$, $p = 0.009$)—but not right dlPFC ($\beta = 0.03$), dACC ($\beta = 0.20$), or rACC ($\beta = -0.05$) (all p's > 0.15)—was a significant negative predictor of the Flanker interference accuracy effect (Figure 1d). The correlations involving the left ($r = -0.30$, $p = 0.007$) and right ($r = -0.04$, $p = 0.71$) dlPFC gamma activity were different only at a trend level ($z = -1.72$, $p = 0.085$). Models for theta and alpha yielded no effects (p's > 0.05).

Specificity analysis. The relationship between gamma current density in the left dlPFC and the Flanker interference effect was confirmed when accounting for (1) current depressive symptoms ($\beta = -0.32$, $p < 0.009$) and (2) neuroticism and reward learning ($\beta = -0.30$, $p = 0.020$).

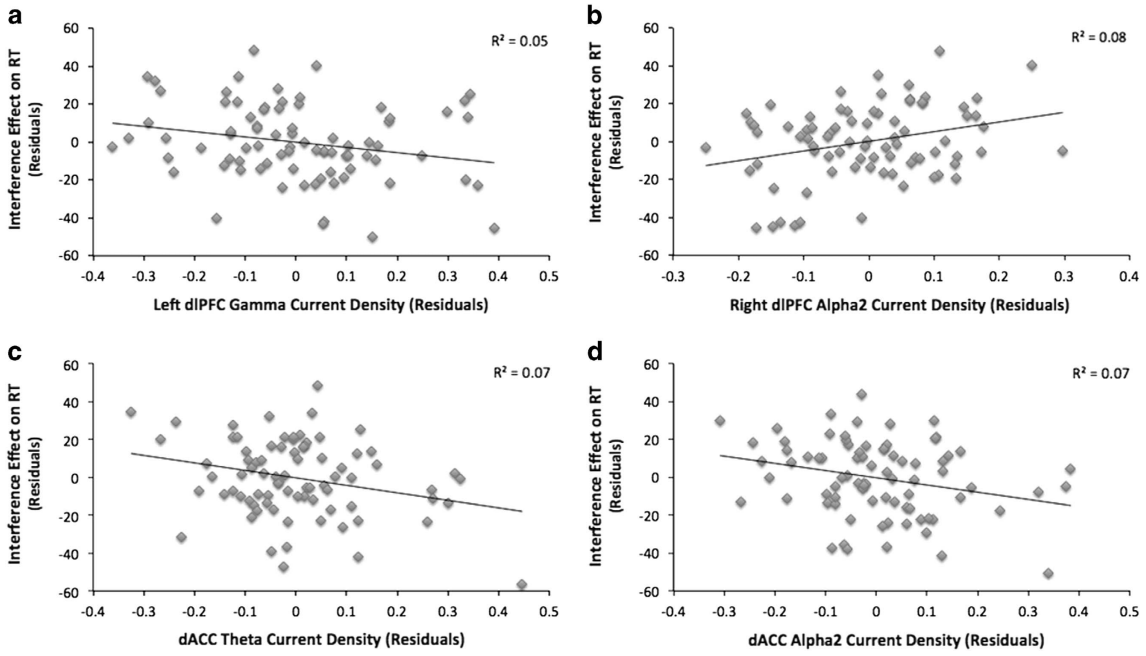

Figure 2 Partial regression plots displaying the association between Flanker interference effect on reaction time (RT) and (a) gamma current density in left dlPFC, after controlling for model covariates (site and gamma activity in the right dlPFC, BA 24'/32' (dACC) and BA 24/32 (rACC), (b) alpha2 current density in the right dlPFC, controlling for site and alpha2 activity in the left dlPFC, dACC, and rACC, (c) theta current density in dACC, controlling for theta activity in rACC, and left and right dlPFC, and (d) alpha2 current density in dACC, controlling for alpha2 activity in rACC, and left and right dlPFC. The theta dACC effect is reduced to a trend level ($\beta = -0.29$, $p = 0.060$) in the model after removing the residual value at the bottom right corner of panel c. It should be noted that the zero-order correlation (ie, excluding model covariates) between theta dACC and interference effect on RT is significant ($r = -0.25$; $p = 0.026$).

Table 1 Whole-Brain Correlations between Candidate Endophenotypes and LORETA-Estimated Current Density

Covariate	Region (frequency band)	Number of voxels	Peak-*r* MNI coordinates			Mean *r*
			x	*y*	*z*	
Neuroticism	Bilateral OFC/sgACC (γ)	36	11	31	−27	0.27*
Reward learning	L dlPFC/OFC (γ)	51	−38	52	8	0.38***
Flanker ACC	L dlPFC (γ)	4	−38	38	36	−0.38***

Abbreviations: dlPFC, dorsolateral prefrontal cortex; OFC, orbitofrontal cortex; sgACC, subgenual anterior cingulate cortex; γ, Gamma (36.5–44 Hz).
For each cluster, the number of voxels exceeding the statistical threshold is reported (using the 'Randomise' permutation-based inference tool in FSL for nonparametric statistical thresholding, with 5000 permutations, $p < 0.05$, FWE corrected for multiple comparisons; Winkler *et al*, 2014); Neuroticism = NEO Five-Factor Inventory (Neuroticism total score); Reward Learning = Change in response bias scores from block 1 to block 2 in the Probabilistic Reward Task; Flanker ACC = Flanker interference effect on accuracy. Peak-r MNI coordinates = MNI coordinates for the voxel associated with the largest Pearson's correlation between the covariate and current density (unit: amperes per square meter, A/m^2); Mean *r* = the mean Pearson's *r* averaged across all voxels belonging to the cluster. Similar to the analyses above, site is included as a covariate.
*$p < 0.05$, ***$p < 0.001$ (uncorrected).

Flanker interference effect (RT). When considering gamma, only current density in the left dlPFC was a negative predictor of interference RT effects ($\beta = -0.23$, $p = 0.045$; Figure 2a). For theta, only dACC activity was negatively associated with the interference RT effect ($\beta = -0.33$, $p = 0.019$; Figure 2c). For alpha2, dACC activity was negatively associated ($\beta = -0.31$, $p = 0.020$) and right dlPFC activity positively associated ($\beta = 0.51$, $p = 0.012$), with the interference effect (Figure 2b and d). All other predictors were nonsignificant (p's > 0.05).

Specificity analysis. The above relationships were confirmed when accounting for (1) current depressive symptoms (theta dACC: $\beta = -0.34$, $p = 0.018$; alpha2 dACC: $\beta = -0.34$, $p = 0.012$; alpha2 right dlPFC: $\beta = 0.58$, $p = 0.005$), with the exception of gamma activity in the left dlPFC ($\beta = -0.22$, $p = 0.054$), and (2) neuroticism and reward learning (theta dACC: $\beta = -0.32$; gamma left dlPFC: $\beta = -0.32$; alpha2 right dlPFC: $\beta = 0.58$; alpha2 dACC: $\beta = -0.34$, p's < 0.020).

Exploratory Whole-Brain Analyses to Examine Specificity of Findings

For the whole-brain correlations with neuroticism, 36 voxels spanning the bilateral OFC and sgACC/rACC (BA11/47, BA25, BA24) correlated positively with gamma activity

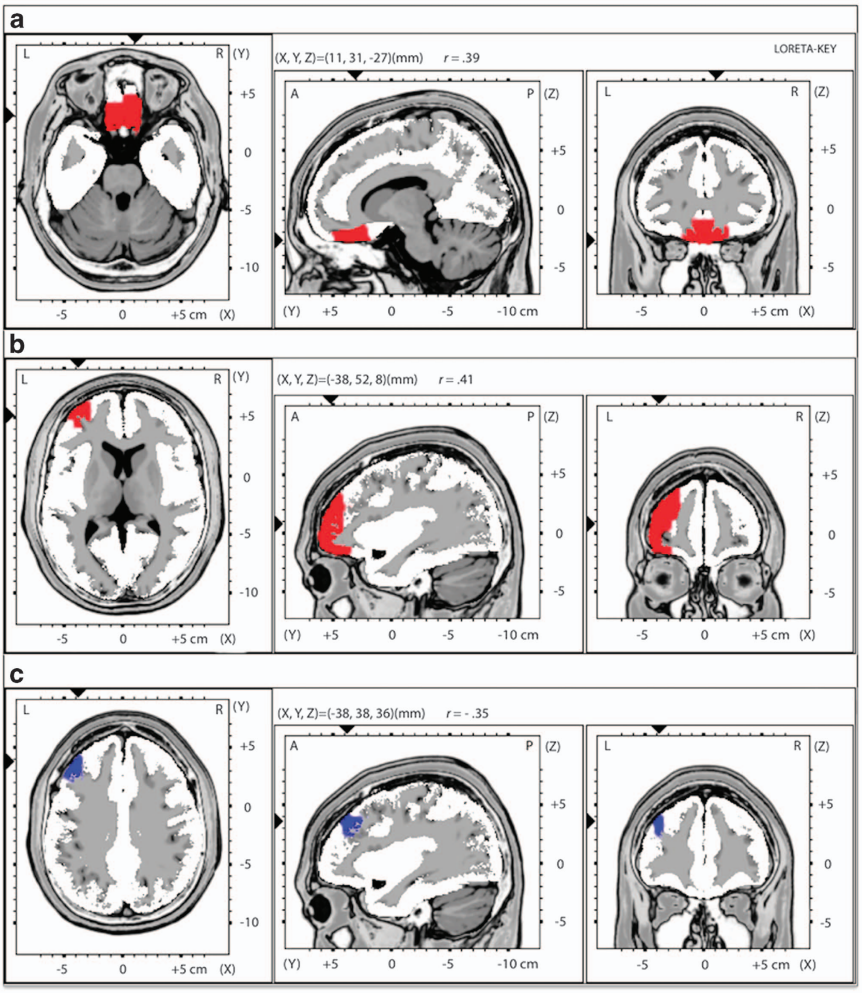

Figure 3 Whole-brain analysis displaying voxel-by-voxel correlations between (a) gamma (36.5–44 Hz) current density and neuroticism (displaying axial/sagittal/coronal views of the bilateral OFC/subgenual ACC cluster (36 voxels) that was significantly positively correlated with neuroticism); (b) gamma current density and reward learning (displaying axial/sagittal/coronal views of the left dlPFC/OFC cluster (51 voxels) that was significantly positively correlated with reward learning); (c) gamma current density and Flanker interference effect on accuracy (displaying axial/sagittal/coronal views of the left dlPFC cluster (4 voxels) that was significantly negatively correlated with the compatibility effect on accuracy).

(Table 1 and Figure 3a). For reward learning, 51 voxels encompassing the left OFC to the dlPFC (including lateral BA10, BA11, BA47, BA9 and BA46) correlated positively with gamma activity (Table 1 and Figure 3b). For the Flanker accuracy interference effect, 4 voxels were significantly negatively correlated with gamma activity (left dlPFC; BA9/10; Table 1 and Figure 3c). For the interference RT effect, no significant effects emerged.

Intercorrelations between Neuroticism, Reward Learning, and Flanker Performance

The three endophenotypes were not significantly intercorrelated (see Supplementary Material).

Cluster Analysis

In an effort to delineate subgroups of depressed patients on the basis of endophenotype profiles, we entered the following standardized variables into a two-step cluster analysis: neuroticism, PRT reward learning scores, and the Flanker accuracy interference effect. A three-cluster solution yielded the best fit (Bayesian Information Criterion = 180.69 and LL = 1.21). The first cluster included 41% ($N = 34$) of the sample, the second cluster 29% ($N = 24$), and the third cluster 28% ($N = 23$). ANOVAs revealed significant differences across clusters in neuroticism ($F(2,78) = 52.39$, $p < 0.001$), reward learning ($F(2,78) = 75.41$, $p < 0.001$), and the interference effect ($F(2,78) = 11.46$, $p < 0.001$). Notably, there were no significant differences across clusters in total HRSD depression scores ($F(2,78) = 1.32$, $p = 0.27$; see Figure 4 for additional details).

DISCUSSION

MDD is increasingly recognized as a highly heterogeneous disorder both in terms of symptom presentation and etiology/pathophysiology. To parse this heterogeneity, there has been increased interest in examining relatively less complex and more tractable endophenotypes. The present study examined whether three promising endophenotypes of

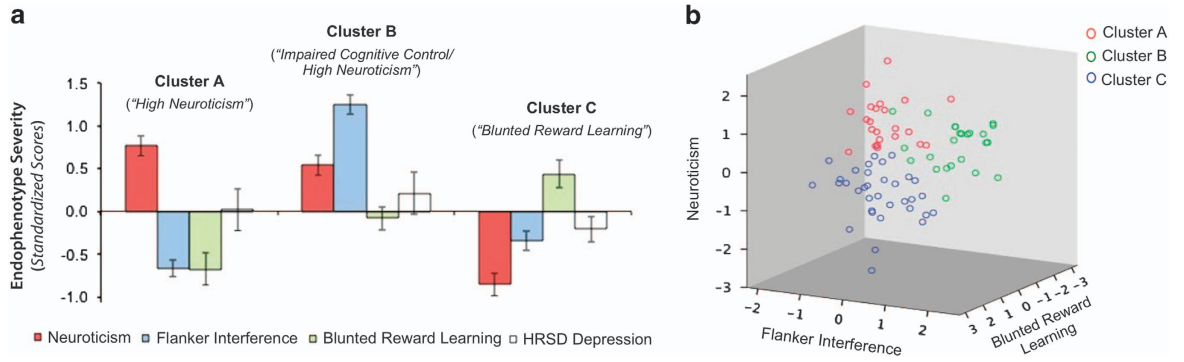

Figure 4 (a) Standardized means (with standard error bars) are displayed for neuroticism (NEO), Flanker interference effect on accuracy, blunted reward learning (PRT), and total depression (HRSD) scores for each of three groups derived from the two-step cluster analysis. (b) Three-dimensional scatterplot displaying association between the three endophenotype variables by cluster group. For consistency across measures, the PRT reward learning variable was reverse scored such that higher scores on each of the displayed measures represent greater severity/impairment.

depression were associated with partially dissociable resting intracranial EEG correlates. To this end, well-validated measures of neuroticism (NEO), reward learning (PRT), and cognitive control (Eriksen Flanker Task) were administered to a sample of depressed adults and correlated with source-localized estimates of resting EEG activity.

Interestingly, the majority of findings emerged in the gamma band. Of note, a combined EEG/FDG-PET study (Oakes *et al*, 2004) revealed that, of all the classic EEG bands, positive correlations between LORETA estimates and resting brain metabolic activity were strongest for gamma. Accordingly, we interpret increased levels of gamma current density as reflecting increased resting brain activity. Here, neuroticism was associated with increased resting gamma current density in a single cluster localized to the OFC and ventral portions of the ACC (ie, subgenual BA25 and rostral BA24). The latter ACC finding partially confirmed our hypotheses. These ventral ACC regions correspond to the 'affective' subdivision of the ACC, which is densely interconnected with limbic and paralimbic structures (eg, amygdala, nucleus accumbens), has been implicated in emotion expression/regulation, and is a critical hub in the default mode network linked to self-referential processing (Buckner *et al*, 2008; Etkin *et al*, 2011). Previous fMRI studies have associated elevated neuroticism with ACC activity (Haas *et al*, 2007; Servaas *et al*, 2013). One study (Haas *et al*, 2007) observed that greater neuroticism correlated with elevated subgenual ACC activation in a nonclinical sample engaged in an emotional conflict task. Our findings extend these reports by showing that neuroticism was associated with elevated subgenual and ventral ACC gamma activity during rest among an unmedicated MDD sample, suggesting that depressed subjects with elevated neuroticism might engage in maladaptive self-referential processing.

Studies probing the neural substrates of neuroticism must contend with potential confounding variables, including current depressive symptoms and related personality variables. Indeed, neuroticism has been repeatedly shown to covary with current depressive symptoms (Klein *et al*, 2011), which, in turn, have been associated with hyperactivity in ventral ACC regions (Gotlib *et al*, 2005; Siegle *et al*, 2007). In an effort to disentangle trait neuroticism effects from the latter confounds, we controlled for current depressive symptoms and the other four NEO factors. Notably, the neuroticism-ACC gamma association remained significant, suggesting that it more likely reflects the trait-like aspects of neuroticism, rather than current depressive symptoms or related personality trait confounds.

The neuroticism-OFC association was not anticipated. However, neuroticism has previously been linked to both reduced cortical thickness (Rauch *et al*, 2005; Wright *et al*, 2006) and gray matter volume (Kringelbach and Rolls, 2004) in the OFC. Moreover, in addition to its role in value encoding, the OFC has been implicated in emotional processing and regulation/expression (Goodkind *et al*, 2012; Rolls and Grabenhorst, 2008). In spite of parallels with prior reports, the current link between OFC function and neuroticism awaits replication.

Our hypotheses regarding reward learning were partially supported. Specifically, blunted reward learning was associated with reduced gamma activity in the left dlPFC and OFC. Highlighting specificity, these associations remained significant when controlling for current depressive symptoms and discriminability (an index of task difficulty). Interestingly, gamma OFC also emerged as a significant predictor of participants' sensitivity to rewards, as derived from computational modeling of trial-by-trial PRT performance. Prior research has implicated both the OFC (Hornak *et al*, 2004; O'Doherty, 2004) and left dlPFC (Ahn *et al*, 2013; Pizzagalli *et al*, 2005b) in reward learning. In a prior study using a different task, blunted reward responsiveness was associated with reduced resting OFC and *left* dlPFC activity among healthy controls (Pizzagalli *et al*, 2005b). However, in contrast to the present study, the latter findings emerged in the alpha2, rather than gamma, frequency band. More recent research has implicated gamma activity in reward processing (Marco-Pallarés *et al*, 2015). Contrary to our hypotheses, resting dACC activity was not associated with reward learning across any EEG band examined.

With regards to cognitive control, greater Flanker interference accuracy effects were associated with reduced left dlPFC gamma power. When decomposing this effect, we found that reduced left dlPFC gamma correlated with lower accuracy for incongruent ($r = 0.35$, $p = 0.001$), but not congruent ($r = 0.08$, $p = 0.440$), trials. [Although these findings highlight specificity, it is important to emphasize that variance in accuracy was reduced for the congruent (SD = 0.02), relative to the incongruent (SD = 0.13), trials, which

may have limited the ability to detect a significant association between LORETA current density and accuracy on congruent trials.] Similarly, left dlPFC gamma activity was negatively associated with interference RT effects. The dlPFC has been strongly implicated in cognitive control (Pizzagalli, 2011; Ridderinkhof *et al*, 2004) and previous studies have linked the left, but not right, dlPFC with cognitive control (MacDonald *et al*, 2000), including studies using the Flanker task (Fassbender *et al*, 2006). In contrast to these findings from task-related fMRI paradigms, the current results indicate that greater *resting* left dlPFC activity predicts performance on a cognitive control task. Within our ROI—but not whole-brain—analyses, increased alpha2 activity in the right dlPFC and decreased theta and alpha2 activity in the dACC were each associated with greater interference RT effects. Because the theta and alpha2 effects were not confirmed in whole-brain analyses, replications are warranted. Importantly, most findings remained significant when controlling for current depressive symptoms and the other endophenotypes.

With regards to our gamma findings, there is evidence that gamma oscillations may facilitate cortical circuit performance and enhance information transmission by increasing signal-to-noise ratio within neocortical circuits (Sohal *et al*, 2009). Although speculative, it is possible that the latter mechanism partially explains the observed findings (eg, greater gamma activity in the left dlPFC reflects relatively enhanced cortical circuit performance in this region, which in turn predicts improved cognitive control performance on the Flanker).

The candidate endophenotypes examined in the current study are themselves complex and multifaceted constructs, which can be parsed into subcomponents. For example, neuroticism has been defined with terms ranging from temperamental, worrying, insecure, and self-conscious (although most, if not all, personality theorists agree that negative emotionality is a defining component; McCrae and Costa, 1987). Similarly, cognitive control is an umbrella term encompassing a range of related abilities, including the ability to *inhibit* automatic or prepotent responses, *shift* in a flexible manner between tasks or mental sets, and *update working memory* in order to retain only relevant information (Friedman *et al*, 2008; Snyder, 2013). Thus, fruitful findings may emerge from studies examining whether different subcomponents of promising endophenotypes have at least partially dissociable neurobiological signatures.

It is also important to highlight that these endophenotypes are not unique to MDD, but rather cut across several DSM diagnostic categories. Thus, it will be important to investigate the transdiagnostic value of candidate endophenotypes by examining their neurobiological and genetic substrates across psychiatrically heterogeneous samples. The current study exclusively focused on MDD given that we were specifically interested in exploring whether the well-documented heterogeneity in this disorder category mapped onto, at least partially, dissociable neural circuitry.

The extent to which these candidate endophenotypes have diagnostic or clinical utility remains an open question. With regards to the present data, an exploratory cluster analysis indicated that three subgroups of depressed patients could be differentiated on the basis of endophenotype profiles, including a subgroup with relatively elevated neuroticism, another with greater impairments in cognitive control, and a final group with relatively blunted reward learning (Figure 4). Although speculative, knowledge of endophenotype profiles may ultimately help inform optimal treatment selection. For example, depressed individuals with impaired cognitive control may benefit from interventions with pro-cognitive effects (eg, vortioxetine, Mahableshwarkar *et al*, 2015). Similarly, certain pharmacological (eg, bupropion) and psychotherapeutic (eg, behavioral activation; Dichter *et al*, 2009) interventions may be particularly beneficial for those depressed individuals characterized by blunted reward learning and reward-circuitry deficits.

Limitations

Several limitations of the present study should be noted. First, EEG source localization techniques cannot adequately probe subcortical structures (eg, amygdala, caudate). Although EEG has the benefits of being non-invasive and relatively inexpensive, and thus may be relatively more practical as a diagnostic tool in future clinical settings, it will be important for subsequent studies examining the neural correlates of plausible MDD endophenotypes to employ modalities with greater spatial resolution (eg, fMRI), as well as the ability to probe networks (eg, DMN, salience network). Second, our findings were primarily in the gamma band. There is some evidence suggesting that current density in higher bands (eg, gamma and beta) may be contaminated by muscle or EMG artifacts (Whitham *et al*, 2007). Although the influence of muscle activity cannot be ruled out, we believe it is unlikely that the current gamma findings (which emerged from resting, task-free EEG data) are due to muscle activity owing to their specificity in terms of hypothesized hemispheric laterality and conditions. Finally, nicotine dependence was not exclusionary, which may represent a possible confound (eg, due to nicotine's possible effects on cognitive and reward function).

FUNDING AND DISCLOSURE

The EMBARC study was supported by the National Institute of Mental Health of the National Institutes of Health under award numbers U01MH092221 (Trivedi, M.H.) and U01MH092250 (McGrath, P.J., Parsey, R.V., Weissman, M. M.). The content is solely the responsibility of the authors and does not necessarily represent the official views of the National Institutes of Health. Drs. Webb, Dillon and Pizzagalli were supported by NIMH F32 MH099801, R00 MH094438, and R01 MH068376, respectively. Valeant Pharmaceuticals donated the Wellbutrin XL used in the study. This work was supported by the EMBARC National Coordinating Center at UT Southwestern Medical Center to Madhukar H. Trivedi, M.D., Coordinating PI, and the Data Center at Columbia and Stony Brook Universities. Dr Kurian has received grant support from the following additional sources: Targacept, Inc.; Pfizer, Inc.; Johnson & Johnson; Evotec; Rexahn; Naurex; and Forest Pharmaceuticals. Dr Trombello owns Merck and J&J stock. Dr Trivedi is or has been an advisor/consultant to: Abbott Laboratories, Inc., Abdi Ibrahim, Akzo (Organon Pharmaceuticals Inc.), Alkermes, AstraZeneca, Axon Advisors, Bristol-Myers Squibb Company, Cephalon, Inc., Cerecor, Concert Pharmaceuticals, Inc., Eli Lilly & Company, Evotec, Fabre Kramer Pharmaceuticals, Inc., Forest Pharmaceuticals,

GlaxoSmithKline, Janssen Global Services, LLC, Janssen Pharmaceutica Products, LP, Johnson & Johnson PRD, Libby, Lundbeck, Meade Johnson, MedAvante, Medtronic, Merck, Mitsubishi Tanabe Pharma Development America, Inc., Naurex, Neuronetics, Otsuka Pharmaceuticals, Pamlab, Parke-Davis Pharmaceuticals, Inc., Pfizer Inc., PgxHealth, Phoenix Marketing Solutions, Rexahn Pharmaceuticals, Ridge Diagnostics, Roche Products Ltd., Sepracor, SHIRE Development, Sierra, SK Life and Science, Sunovion, Takeda, Tal Medical/Puretech Venture, Targacept, Transcept, VantagePoint, Vivus, and Wyeth-Ayerst Laboratories. In addition, he has received research support from: Agency for Healthcare Research and Quality (AHRQ), Corcept Therapeutics, Inc., Cyberonics, Inc., National Alliance for Research in Schizophrenia and Depression, National Institute of Mental Health, National Institute on Drug Abuse, Novartis, Pharmacia & Upjohn, Predix Pharmaceuticals (Epix), and Solvay Pharmaceuticals, Inc. For a comprehensive list of lifetime disclosures of Dr Fava, see http://mghcme.org/faculty/faculty-detail/maurizio_fava. Over the past 3 years, Dr McGrath has received research support from the National Institute of Mental Health, the New York State Department of Mental Hygiene, the Research Foundation for Mental Hygiene (New York State), F. Hoffman-LaRoche, Ltd., Naurex Pharmaceuticals, Forest Research and Sunovion Pharmaceuticals. In the past 3 years, Dr Weissman received funding from the National Institute of Mental Health, the National Institute on Drug Abuse, the National Alliance for Research on Schizophrenia and Depression, the Sackler Foundation, and the Templeton Foundation; and received royalties from the Oxford University Press, Perseus Press, the American Psychiatric Association Press and MultiHealth Systems. Dr Weissman declares that none of these present a conflict of interest. Dr Grannemann declares that, except for income received from a primary employer and the above grant (U01MH092221), no financial support or compensation has been received from any individual or corporate entity over the past 3 years for research or professional service and there are no personal financial holdings that could be perceived as constituting a potential conflict of interest. Over the past 3 years, Dr Pizzagalli has received honoraria/consulting fees from Advanced Neuro Technology North America, AstraZeneca, Otsuka America Pharmaceutical, Pfizer, and Servier for activities unrelated to this project. The remaining authors declare no conflict of interest.

ACKNOWLEDGMENTS

We thank Alex Shackman, PhD, for providing regions-of-interest definition based on anatomical atlases and landmarks. We also thank Steven Lowen, PhD, and Garrett Fitzmaurice, ScD, for their statistical consultation.

REFERENCES

Ahn HM, Kim SE, Kim SH (2013). The effects of high-frequency rTMS over the left dorsolateral prefrontal cortex on reward responsiveness. *Brain Stimulat* **6**: 310–314.

Birley AJ, Gillespie NA, Heath AC, Sullivan PF, Boomsma DI, Martin NG (2006). Heritability and nineteen-year stability of long and short EPQ-R Neuroticism scales. *Personal Individ Differ* **40**: 737–747.

Bogdan R, Pizzagalli DA (2009). The heritability of hedonic capacity and perceived stress: a twin study evaluation of candidate depressive phenotypes. *Psychol Med* **39**: 211–218.

Buckner RL, Andrews-Hanna JR, Schacter DL (2008). The Brain's default network. *Ann NY Acad Sci* **1124**: 1–38.

Chan RCK, Gottesman II (2008). Neurological soft signs as candidate endophenotypes for schizophrenia: A shooting star or a Northern star? *Neurosci Biobehav Rev* **32**: 957–971.

Chiu T, Fang D, Chen J, Wang Y, Jeris C (2001). A robust and scalable clustering algorithm for mixed type attributes in large database environment. *Proc Seventh ACM SIGKDD Int Conf Knowl Discov Data Min* 263–268.

Christensen MV, Kyvik KO, Kessing LV (2006). Cognitive function in unaffected twins discordant for affective disorder. *Psychol Med* **36**: 1119–1129.

Costa PT, Bagby RM, Herbst JH, McCrae RR (2005). Personality self-reports are concurrently reliable and valid during acute depressive episodes. *J Affect Disord* **89**: 45–55.

Dichter GS, Felder JN, Petty C, Bizzell J, Ernst M, Smoski MJ (2009). The effects of psychotherapy on neural responses to rewards in major depression. *Biol Psychiatry* **66**: 886–897.

Eriksen BA, Eriksen CW (1974). Effects of noise letters upon the identification of a target letter in a nonsearch task. *Percept Psychophys* **16**: 143–149.

Etkin A, Egner T, Kalisch R (2011). Emotional processing in anterior cingulate and medial prefrontal cortex. *Trends Cogn Sci* **15**: 85–93.

Farmer A, Redman K, Harris T, Mahmood A, Sadler S, Pickering A *et al* (2002). Neuroticism, extraversion, life events and depression. The Cardiff Depression Study. *Br J Psychiatry* **181**: 118–122.

Fassbender C, Foxe JJ, Garavan H (2006). Mapping the functional anatomy of task preparation: Priming task-appropriate brain networks. *Hum Brain Mapp* **27**: 819–827.

Fava GA, Guidi J, Porcelli P, Rafanelli C, Bellomo A, Grandi S *et al* (2012). A cluster analysis-derived classification of psychological distress and illness behavior in the medically ill. *Psychol Med* **42**: 401–407.

Friedman NP, Miyake A, Young SE, DeFries JC, Corley RP, Hewitt JK (2008). Individual differences in executive functions are almost entirely genetic in origin. *J Exp Psychol Gen* **137**: 201–225.

De Fruyt F, Leeuwen K, Van, Bagby RM, Rolland J-P, Rouillon F (2006). Assessing and interpreting personality change and continuity in patients treated for major depression. *Psychol Assess* **18**: 71–80.

Goldstein BL, Klein DN (2014). A review of selected candidate endophenotypes for depression. *Clin Psychol Rev* **34**: 417–427.

Goodkind MS, Sollberger M, Gyurak A, Rosen HJ, Rankin KP, Miller B *et al* (2012). Tracking emotional valence: the role of the orbitofrontal cortex. *Hum Brain Mapp* **33**: 753–762.

Gotlib IH, Sivers H, Gabrieli JDE, Whitfield-Gabrieli S, Goldin P, Minor KL *et al* (2005). Subgenual anterior cingulate activation to valenced emotional stimuli in major depression. *Neuroreport* **16**: 1731–1734.

Gottesman II, Gould TD (2003). The endophenotype concept in psychiatry: etymology and strategic intentions. *Am J Psychiatry* **160**: 636–645.

Haas BW, Omura K, Constable RT, Canli T (2007). Emotional conflict and neuroticism: Personality-dependent activation in the amygdala and subgenual anterior cingulate. *Behav Neurosci* **121**: 249–256.

Hamilton M (1960). A rating scale for depression. *J Neurol Neurosurg Psychiatry* **23**: 56–62.

Holmes AJ, Bogdan R, Pizzagalli DA (2010). Serotonin transporter genotype and action monitoring dysfunction: a possible substrate underlying increased vulnerability to depression. *Neuropsychopharmacology* **35**: 1186–1197.

Hornak J, O'doherty J, Bramham J, Rolls ET, Morris RG, Bullock PR *et al* (2004). Reward-related reversal learning after

surgical excisions in orbito-frontal or dorsolateral prefrontal cortex in humans. *J Cogn Neurosci* **16**: 463–478.

Huys QJ, Pizzagalli DA, Bogdan R, Dayan P (2013). Mapping anhedonia onto reinforcement learning: a behavioural meta-analysis. *Biol Mood Anxiety Disord* **3**: 12.

Kendler K, Gatz M, Gardner CO, Pedersen NL (2006). Personality and major depression: A swedish longitudinal, population-based twin study. *Arch Gen Psychiatry* **63**: 1113–1120.

Klein DN, Kotov R, Bufferd SJ (2011). Personality and depression: explanatory models and review of the evidence. *Annu Rev Clin Psychol* **7**: 269–295.

Kringelbach ML, Rolls ET (2004). The functional neuroanatomy of the human orbitofrontal cortex: evidence from neuroimaging and neuropsychology. *Prog Neurobiol* **72**: 341–372.

MacDonald AW, Cohen JD, Stenger VA, Carter CS (2000). Dissociating the role of the dorsolateral prefrontal and anterior cingulate cortex in cognitive control. *Science* **288**: 1835–1838.

Mahableshwarkar AR, Zajecka J, Jacobson W, Chen Y, Keefe RS (2015). A randomized, placebo-controlled, active-reference, double-blind, flexible-dose study of the efficacy of vortioxetine on cognitive function in major depressive disorder. *Neuropsychopharmacology* **40**: 2025–2037.

Marco-Pallarés J, Münte TF, Rodríguez-Fornells A (2015). The role of high-frequency oscillatory activity in reward processing and learning. *Neurosci Biobehav Rev* **49**: 1–7.

McCrae RR, Costa PT (1987). Validation of the five-factor model of personality across instruments and observers. *J Pers Soc Psychol* **52**: 81–90.

McCrae RR, Costa PT (2010). NEO Inventories for the NEO Personality Inventory-3 (NEO-PI-3), NEO Five-Factor Inventory-3 (NEO-FFI-3), NEO Personality Inventory-Revised (NEO PI-R): Professional Manual. PAR: Lutz, FL.

Meng X, Rosenthal R, Rubin DB (1992). Comparing correlated correlation coefficients. *Psychol Bull* **111**: 172–175.

Modell S, Huber J, Holsboer F, Lauer CJ (2003). The Munich Vulnerability Study on Affective Disorders: risk factors for unipolarity versus bipolarity. *J Affect Disord* **74**: 173–184.

Oakes TR, Pizzagalli DA, Hendrick AM, Horras KA, Larson CL, Abercrombie HC *et al* (2004). Functional coupling of simultaneous electrical and metabolic activity in the human brain. *Hum Brain Mapp* **21**: 257–270.

O'Doherty JP (2004). Reward representations and reward-related learning in the human brain: insights from neuroimaging. *Curr Opin Neurobiol* **14**: 769–776.

Ouimette PC, Klein DN, Pepper CM (1996). Personality traits in the first degree relatives of outpatients with depressive disorders. *J Affect Disord* **39**: 43–53.

Pascual-Marqui RD, Lehmann D, Koenig T, Kochi K, Merlo MCG, Hell D *et al* (1999). Low resolution brain electromagnetic tomography (LORETA) functional imaging in acute, neuroleptic-naive, first-episode, productive schizophrenia. *Psychiatry Res Neuroimaging* **90**: 169–179.

Pechtel P, Dutra SJ, Goetz EL, Pizzagalli DA (2013). Blunted reward responsiveness in remitted depression. *J Psychiatr Res* **47**: 1864–1869.

Pizzagalli DA (2011). Frontocingulate dysfunction in depression: toward biomarkers of treatment response. *Neuropsychopharmacology* **36**: 183–206.

Pizzagalli DA (2014). Depression, stress, and anhedonia: toward a synthesis and integrated model. *Annu Rev Clin Psychol* **10**: 393–423.

Pizzagalli DA, Evins AE, Schetter EC, Frank MJ, Pajtas PE, Santesso DL *et al* (2008). Single dose of a dopamine agonist impairs reinforcement learning in humans: Behavioral evidence from a laboratory-based measure of reward responsiveness. *Psychopharmacology (Berl)* **196**: 221–232.

Pizzagalli DA, Jahn AL, O'Shea JP (2005a). Toward an objective characterization of an anhedonic phenotype: a signal-detection approach. *Biol Psychiatry* **57**: 319–327.

Pizzagalli DA, Sherwood RJ, Henriques JB, Davidson RJ (2005b). Frontal brain asymmetry and reward responsiveness a source-localization study. *Psychol Sci* **16**: 805–813.

Rauch SL, Milad MR, Orr SP, Quinn BT, Fischl B, Pitman RK (2005). Orbitofrontal thickness, retention of fear extinction, and extraversion. *Neuroreport* **16**: 1909–1912.

Ridderinkhof KR, van den, Wildenberg WPM, Segalowitz SJ, Carter CS (2004). Neurocognitive mechanisms of cognitive control: the role of prefrontal cortex in action selection, response inhibition, performance monitoring, and reward-based learning. *Brain Cogn* **56**: 129–140.

Rolls ET, Grabenhorst F (2008). The orbitofrontal cortex and beyond: from affect to decision-making. *Prog Neurobiol* **86**: 216–244.

Rush AJ, Trivedi MH, Ibrahim HM, Carmody TJ, Arnow B, Klein DN *et al* (2003). The 16-Item quick inventory of depressive symptomatology (QIDS), clinician rating (QIDS-C), and self-report (QIDS-SR): a psychometric evaluation in patients with chronic major depression. *Biol Psychiatry* **54**: 573–583.

Rushworth MF, Buckley MJ, Behrens TE, Walton ME, Bannerman DM (2007). Functional organization of the medial frontal cortex. *Curr Opin Neurobiol* **17**: 220–227.

Santesso DL, Dillon DG, Birk JL, Holmes AJ, Goetz E, Bogdan R *et al* (2008). Individual differences in reinforcement learning: behavioral, electrophysiological, and neuroimaging correlates. *NeuroImage* **42**: 807–816.

Sarapas C, Shankman SA, Harrow M, Goldberg JF (2012). Parsing trait and state effects of depression severity on neurocognition: evidence from a 26-year longitudinal study. *J Abnorm Psychol* **121**: 830–837.

Servaas MN, Velde J, van der, Costafreda SG, Horton P, Ormel J, Riese H *et al* (2013). Neuroticism and the brain: a quantitative meta-analysis of neuroimaging studies investigating emotion processing. *Neurosci Biobehav Rev* **37**: 1518–1529.

Siegle G, Ghinassi F, Thase M (2007). Neurobehavioral therapies in the 21st century: summary of an emerging field and an extended example of cognitive control training for depression. *Cogn Ther Res* **31**: 235–262.

Snyder HR (2013). Major depressive disorder is associated with broad impairments on neuropsychological measures of executive function: a meta-analysis and review. *Psychol Bull* **139**: 81–132.

Sohal VS, Zhang F, Yizhar O, Deisseroth K (2009). Parvalbumin neurons and gamma rhythms enhance cortical circuit performance. *Nature* **459**: 698–702.

Stins JF, Baal GCM, van, Polderman TJ, Verhulst FC, Boomsma DI (2004). Heritability of Stroop and flanker performance in 12-year old children. *BMC Neurosci* **5**: 49.

Whitham EM, Pope KJ, Fitzgibbon SP, Lewis T, Clark CR, Loveless S *et al* (2007). Scalp electrical recording during paralysis: quantitative evidence that EEG frequencies above 20 Hz are contaminated by EMG. *Clin Neurophysiol* **118**: 1877–1888.

Winkler AM, Ridgway GR, Webster MA, Smith SM, Nichols TE (2014). Permutation inference for the general linear model. *NeuroImage* **92**: 381–397.

Wöstmann NM, Aichert DS, Costa A, Rubia K, Möller H-J, Ettinger U (2013). Reliability and plasticity of response inhibition and interference control. *Brain Cogn* **81**: 82–94.

Wright CI, Williams D, Feczko E, Barrett LF, Dickerson BC, Schwartz CE *et al* (2006). Neuroanatomical correlates of extraversion and neuroticism. *Cereb Cortex* **16**: 1809–1819.

Supplementary Information accompanies the paper on the Neuropsychopharmacology website (http://www.nature.com/npp)

Supplemental Material

Neural Correlates of Three Promising Endophenotypes of Depression: Evidence from the EMBARC Study

Supplemental Methods and Materials

Participants. In addition to the criteria listed in the main text, patients were excluded if they failed to respond to an adequate trial of an antidepressant in the current episode, or if they received treatment with ECT, VNS, rTMS or other somatic treatments in the current episode. For the present sample, mean age of first MDE was 16.2 (SD = 6.1), with a median number of prior MDEs of 6.0 (median length of current episode = 12 months). Ten percent (n=8) of the sample met criteria for current Panic Disorder; 7% (n=6) for PTSD; 12% (n=10) for GAD and 15% (n=12) for Social Phobia.

EEG Band Selection. Consistent with prior EEG source localization studies (Pizzagalli *et al*, 2006), analyses probing the ACC focused on the theta (6.5–8 Hz) and gamma (36.5–44 Hz) bands. The focus on these bands is justified on the basis of human and animal findings indicating that the ACC plays a critical role in the generation and/or modulation of theta activity (Cavanagh and Frank, 2014; Debener *et al*, 2005; Phillips *et al*, 2013; Tsujimoto *et al*, 2010; Womelsdorf *et al*, 2010), and that theta and gamma activity are functionally coupled (Burgess and Ali, 2002; Canolty *et al*, 2006; Düzel *et al*, 2003; Fell *et al*, 2003; Hajos *et al*, 2003; Schack *et al*, 2002). Further supporting the examination of gamma current density, a prior study (Oakes *et al*, 2004) found that the strongest positive correlations between resting brain metabolic activity (FDG-PET) and intracranial estimates of standard EEG bands emerged for the gamma (36.5–44 Hz)

frequency range. Moreover, gamma activity has been strongly implicated in reward processing (see Marco-Pallarés *et al*, 2015). In addition, both theta and gamma have been implicated in cognitive control (Cavanagh and Frank, 2014; Cavanagh and Shackman, 2014; Pizzagalli *et al*, 2006) and neuroticism (Jaušovec and Jaušovec, 2007; Neo and McNaughton, 2011). It is important to note that the bulk of this research has focused on task-induced EEG activity (e.g., theta activity generated during cognitive control tasks, gamma activity induced during working memory and selective attention tasks). However, previous studies have observed associations between resting gamma activity and both neuroticism (Jaušovec, & Jaušovec, 2007) and cognitive control (e.g., post-error adjustment on the Flanker task; Pizzagalli et al., 2006). Thus, to be consistent with previous relevant LORETA studies, and to facilitate comparison of findings, our investigation of gamma current density was restricted to 36.5-44hz (e.g., see Mueller *et al*, 2014; Oakes *et al*, 2004; Wacker *et al*, 2009). Finally, given prior research implicating resting alpha band activity in reward learning (Pizzagalli *et al*, 2005), we also examined current density in the alpha1 (8.5-10 Hz) and alpha2 (10.5–12 Hz) frequency range.

Probabilistic Reward Task. In this task, which is rooted in signal detection theory, subjects were asked to determine, via button press, whether one of two stimuli was presented on the screen: a short (11.5 mm) or a long (13 mm) mouth, superimposed on a previously mouthless cartoon face. In the present study, two blocks consisting of 100 trials were presented. Within each block an equal number of short and long mouths were presented. Each trial consisted of a fixation cross (jittered 750-900 ms) followed by a mouthless face (500 ms), after which either the short or a long mouth appeared on the face (100 ms). Importantly, to induce a response bias, an asymmetric reinforcer ratio was employed. Namely, correct identification of either the long or short mouth was rewarded (“Correct!! You won 5 Cents”) three times more frequently (“rich”

stimulus) than the other mouth ("lean" stimulus). Participants were informed at the beginning of the task that the purpose of the game was to win as much money as possible, but that not every correct response would yield reward feedback. Keys and conditions (long or short mouth as "rich" stimulus) were counterbalanced across participants. Participants were excluded if any of the following quality control checks were not met: (1) less than 80 valid trials in each block (i.e., less than 20% outlier responses, as defined by RT shorter than 150 ms or greater than 2,500 ms and the log-transformed RT exceeding the participant's mean±3SD; see [Pizzagalli *et al.*, 2008] for more detail); (2) less than 24 rich rewards or less than 7 lean rewards in each block; (3) rich-to-lean reward ratio < 2.5 in any block; and (4) rich or lean accuracy < 0.40 in any block.

RB scores – our main variable of interest – capture a participant's preference for the most frequently rewarded ("rich") stimulus, and were calculated as (Pizzagalli *et al*, 2008):

$$\log b = 0.5*\log\{[(Rich_{Correct}+0.5) * (Lean_{Incorrect}+0.5)]/ [(Rich_{Incorrect}+0.5) * (Lean_{Correct}+0.5)]\}.$$

In addition, *discriminability* scores, indexing the ability to differentiate between the two stimuli, were included as a covariate in specificity analyses. Consistent with prior research, discriminability was calculated as (Pizzagalli *et al*, 2008):

$$\log d = 0.5*\log\{[(Rich_{Correct}+0.5) * (Lean_{Correct}+0.5)]/ [(Rich_{Incorrect}+0.5) * (Lean_{Incorrect}+0.5)]\}.$$

Computational Modeling. A series of reinforcement-learning models were fitted to the PRT choice data (see Huys *et al*, 2013). These models tested whether subjects associated rewards with stimulus-action pairs, with actions, or with a mixture of the two stimulus-action associations weighted by an uncertainty factor. They also tested whether subjects treated zero outcomes as losses. The models were fitted using an empirical Bayesian random-effects approach and were

compared using integrated group-level BIC factors following previously established procedures (Huys *et al*, 2013). All sessions were fitted at once, meaning that individual subject parameter inference was constrained by an empirical prior distribution, i.e., a prior that was in turn inferred from all the data. No further assumptions were made and all sessions were treated equally.

There was no evidence that subjects treated zero outcomes as losses. A model in which the rewarding outcomes were associated purely with actions gave the most parsimonious account of the data ($\log_{10}\Delta$iBIC compared to second-most parsimonious model > 100 which is decisive evidence in favor of the better fitting model). This model had four parameters. Reward sensitivity (mean; 1.84, SD: 0.89) measured the immediate behavioral impact of rewards. Learning rate (mean: 0.16, SD: 0.22) measured subjects' ability to accumulate rewards over time and hence to learn from the rewards. Instruction sensitivity (mean: 1.49, SD: 0.64) measured subjects' tendency to follow the instructions (i.e., which response to press for which stimulus). Initial bias (mean: -0.11, SD: 0.07) measured subjects' initial bias towards one response or the other. The present study focused on the reward sensitivity and learning rate parameters.

Eriksen Flanker Task. Participants first completed a practice session consisting of 15 congruent and 15 incongruent trials. The flanking arrows were first presented alone (100 ms) and were then joined by the central arrow (50 ms), for a total stimulus duration of 150 ms. Participants were asked to indicate, via button press, whether the center arrow pointed left or right. Both accuracy and reaction time (RT) were recorded. Following the practice session, participants completed five blocks consisting of 70 trials each (46 congruent, 24 congruent), for a total of 350 trials. To ensure adequate task difficulty, a response deadline was established for each block that corresponded to the 85th percentile of the RT distribution from incongruent trials in the preceding block (in the first block, the practice RT distribution was used). Stimulus

presentation was followed by a fixation cross (1400 ms). If the participant did not respond by the response deadline, a screen reading “TOO SLOW!” was presented (300 ms). Participants were told that if they saw this screen, they should speed up. If a response was made before the deadline, the “TOO SLOW!” screen was omitted and the fixation cross remained onscreen for the 300 ms interval. Finally, each trial ended with presentation of the fixation cross for an additional 200-400 ms. Thus, total trial time varied between 2050-2250 ms. The sequence of congruent and incongruent trials was established with optseq2 (http://surfer.nmr.mgh.harvard.edu/optseq/) and was identical across participants.

While data collection was ongoing, block-by-block feedback was added to maintain performance at desired levels. Specifically, if participants made fewer than three incongruent errors in a block, they were shown a screen reading, “Remember to respond as QUICKLY as possible while still being accurate”. If six or more incongruent errors were committed, the screen read, “Remember to respond as ACCURATELY as possible while still being fast”. Otherwise, the screen read, “Please respond as quickly and accurately as possible”.

Quality control checks were used to exclude datasets characterized by unusually poor performance. First, for each participant outlier trials were defined as those in which the raw RT was less than 150 ms or the log-transformed RT exceeded the participant’s mean±3SD, computed separately for congruent and incongruent stimuli. Second, we excluded datasets with: 35 or more RT outliers (i.e., greater than 10% of trials), fewer than 200 outlier-free congruent trials, fewer then 90 outlier-free incongruent trials, or lower than 50% correct for congruent or incongruent trials. Trials characterized by RT outliers were excluded from all analyses. Data from 82 subjects passed both the Flanker and PRT checks and constitute the final sample.

EEG Acquisition Methods

Intersite Standardization. Staff responsible for administering EEG sessions used the same pre-written set of instructions, and were certified, via videoconference, by the CU site after demonstrating: 1) proper EEG cap placement, 2) accurate administration of task instructions and 3) submitting satisfactory EEG data from a practice administration with a volunteer. The EEG data were acquired using different recording equipment at each of the four study sites (CU, TX, UM, MGH). To maximize intersite comparability, the location of the recording electrode montage was optimized in all cases using direct measurements of electrode locations corresponding 10-20 system landmarks (nasion, inion, auditory meatus, vertex). Below, we describe the EEG acquisition methods at each site.

CU acquisition methods. The electrode montage consisted of 72 expanded 10-20 system scalp channels (Pivik *et al*, 1993) on a Lycra stretch electrode cap (Electro Cap International, Inc.). The cap includes 12 midline sites (nose, Nz to Iz) and 30 homologous pairs over the left and right hemisphere, extending laterally to include the inferior temporal lobes. EEG signals from the Ag/AgCl electrodes were recorded using an active reference (ActiveTwo EEG system) at sites PPO1 (common mode sense) and PPO2 (driven right leg). The scalp placements involved a conventional water soluble electrolyte gel and the interface was verified by the ActiView acquisition software. Additional care was taken to avoid electrolyte bridges (Alschuler *et al*, 2014; Tenke and Kayser, 2001). Continuous EEG was acquired at 256 samples/s using the 24-bit Biosemi system. Raw data files were saved in the native (.bdf) format.

TX acquisition methods. Fifty-eight expanded 10-20 system scalp channels on a Lycra stretch electrode cap served as the electrode montage. The electrode cap included 8 midline sites (Nz to Iz) and 26 homologous pairs over the left and right hemisphere, extending laterally to

include the two mastoids (recorded using nose reference). Continuous EEG was acquired at 250 samples/s using the 32-bit Neuroscan system. Raw data files were saved in the native (.cnt) format.

UM acquisition methods. Sixty expanded 10-20 system scalp channels on a Lycra stretch electrode cap served as the electrode montage at this site. The montage included 8 midline sites (FPz to Oz) and 26 homologous pairs over the left and right hemisphere, extending laterally to include the two mastoids (recorded using a nose reference). Continuous EEG was acquired at 250 samples/s using the 32-bit Neuroscan system. Raw data files were saved in the native (.cnt) format.

MGH acquisition methods. EEG acquisition for the MGH site took place at McLean Hospital. The electrode montage consisted of a 128-channel geodesic net (Electrical Geodesics, Inc.; EGI), including 10 midline sites (Nz to Iz) and 52 homologous pairs over the left and right hemisphere, extending laterally below to include the two mastoids (below the 10-20 landmarks). The montage also included 2 electrodes below each ear and 5 on each side of the face. A Cz reference was employed. The scalp electrodes were prepared using a saline solution, with impedances verified by the Netstation acquisition software, and with particular care taken to optimize the montage based on landmarks of the 10-20 system (nasion, inion, auditory meatus, vertex). Continuous EEG was acquired at 250 samples/s using NetStation software. Raw data files saved in the native (.raw) format.

EEG Preprocessing Methods

EEG data processing was performed at the CU site, whereas LORETA analyses were conducted at McLean Hospital. All EEG data were first converted to BDF format (EEGLAB).

Subsequently, data were converted to the 72-channel CU electrode montage. Specifically, missing channels from the UM and TX data were interpolated using spherical splines (Perrin *et al*, 1989), while all 72 channels were interpolated from the existing 128 channels for the McLean Hospital data. Finally, PolyREX was used to remove DC offsets, optimize data scaling, re-reference to a nose-tip reference, and convert to 16-bit CNT.

The continuous EEG data were blink corrected using a spatial, singular value decomposition (NeuroScan) and segmented into 2-s epochs every .5-s (75% overlap). To aid identification of blinks and eye movements, bipolar EOG recordings (interpolated using spherical splines) were employed. The continuous data were epoched and averaged in a separate process prior to blink correction, and the resulting Hjorth averages were inspected. Epoched data were then screened for electrolyte bridges (Alschuler *et al*, 2014; Tenke and Kayser, 2001). Channels containing artifacts or noise for any given trial were identified using a reference-free approach to identify isolated EEG channels containing amplifier drift, residual eye activity, muscle or movement-related artifacts for any given trial, which were then replaced by spherical spline interpolations from artifact-free channels (i.e., if fewer than 25% of all channels contained artifact). Finally, an automated step was included to reject any remaining epochs exceeding a ±100 μV. Three members of the Columbia University study staff were involved in data cleaning and processing, and each was supervised by Craig E. Tenke, Ph.D

Low Resolution Electromagnetic Tomography (LORETA). LORETA computes intracranial estimates of current density from scalp-recorded EEG data by assuming similar levels of activation among neighboring neurons (no assumption is made about the number of generating sources). LORETA partitions the brain into 2,394 cubic “voxels” (voxel dimension: 7 mm^3) and is limited to cortical gray matter and hippocampi, according to the digitized MNI

probability atlases available from the Montreal Neurologic Institute (MNI; Montreal, Quebec, Canada). This distributed source localization technique has received cross-modal validation from studies combining LORETA with functional MRI (fMRI) (Mulert *et al*, 2004; Vitacco *et al*, 2002), structural MRI (Cannon *et al*, 2011; Worrell *et al*, 2000), intracranial EEG recordings (Zumsteg *et al*, 2005a, 2006) and PET (Pizzagalli *et al*, 2004; Zumsteg *et al*, 2005b), but see (Gamma *et al*, 2004). Consistent with established procedures (Pizzagalli *et al*, 2004), LORETA activity was normalized to a total power of 1 before statistical analyses. To reduce differences across sites, a smoothness parameter of 10^{-5} was used. Mean intensity-normalized current density (averaged across voxels) was extracted from *a priori* regions-of-interest (see Figure S1).

Supplemental Results

Intercorrelations between neuroticism, reward learning and Flanker performance

The three endophenotypes were not significantly inter-correlated: neuroticism - reward learning (r = .15; p = .18), neuroticism - Flanker accuracy and RT (r = .21; p = .055; r = -.14; p = .201, respectively); reward learning - Flanker accuracy and RT (r = -.10; p = .392; r = .04; p = .738, respectively).

Supplemental References

Alschuler DM, Tenke CE, Bruder GE, Kayser J (2014). Identifying electrode bridging from electrical distance distributions: a survey of publicly-available EEG data using a new method. *Clin Neurophysiol Off J Int Fed Clin Neurophysiol* **125**: 484–490.

Burgess AP, Ali L (2002). Functional connectivity of gamma EEG activity is modulated at low frequency during conscious recollection. *Int J Psychophysiol* **46**: 91–100.

Cannon R, Kerson C, Hampshire A (2011). sLORETA and fMRI Detection of Medial Prefrontal Default Network Anomalies in Adult ADHD. *J Neurother* **15**: 358–373.

Canolty RT, Edwards E, Dalal SS, Soltani M, Nagarajan SS, Kirsch HE, *et al* (2006). High Gamma Power Is Phase-Locked to Theta Oscillations in Human Neocortex. *Science* **313**: 1626–1628.

Cavanagh JF, Frank MJ (2014). Frontal theta as a mechanism for cognitive control. *Trends Cogn Sci* **18**: 414–421.

Cavanagh JF, Shackman AJ (2014). Frontal midline theta reflects anxiety and cognitive control: Meta-analytic evidence. *J Physiol-Paris* doi:10.1016/j.jphysparis.2014.04.003.

Debener S, Ullsperger M, Siegel M, Fiehler K, Cramon DY von, Engel AK (2005). Trial-by-Trial Coupling of Concurrent Electroencephalogram and Functional Magnetic Resonance Imaging Identifies the Dynamics of Performance Monitoring. *J Neurosci* **25**: 11730–11737.

Düzel E, Habib R, Schott B, Schoenfeld A, Lobaugh N, McIntosh AR, *et al* (2003). A multivariate, spatiotemporal analysis of electromagnetic time-frequency data of recognition memory. *NeuroImage* **18**: 185–197.

Fell J, Klaver P, Elfadil H, Schaller C, Elger CE, Fernández G (2003). Rhinal–hippocampal theta coherence during declarative memory formation: interaction with gamma synchronization? *Eur J Neurosci* **17**: 1082–1088.

Gamma A, Lehmann D, Frei E, Iwata K, Pascual-Marqui RD, Vollenweider FX (2004). Comparison of simultaneously recorded [H215O]-PET and LORETA during cognitive and pharmacological activation. *Hum Brain Mapp* **22**: 83–96.

Goncharova II, McFarland DJ, Vaughan TM, Wolpaw JR (2003). EMG contamination of EEG: spectral and topographical characteristics. *Clin Neurophysiol* **114**: 1580–1593.

Hajos M, Hoffmann WE, Robinson DD, Yu JH, Hajos-Korcsok E (2003). Norepinephrine but not serotonin reuptake inhibitors enhance theta and gamma activity of the septo-hippocampal system. *Neuropsychopharmacology* **28**: 857–864.

Huys QJ, Pizzagalli DA, Bogdan R, Dayan P (2013). Mapping anhedonia onto reinforcement learning: a behavioural meta-analysis. *Biol Mood Anxiety Disord* **3**: 12.

Jaušovec N, Jaušovec K (2007). Personality, gender and brain oscillations. *Int J Psychophysiol* **66**: 215–224.

Marco-Pallarés J, Münte TF, Rodríguez-Fornells A (2015). The role of high-frequency oscillatory activity in reward processing and learning. *Neurosci Biobehav Rev* **49**: 1–7.

Mueller EM, Panitz C, Hermann C, Pizzagalli DA (2014). Prefrontal Oscillations during Recall of Conditioned and Extinguished Fear in Humans. *J Neurosci* **34**: 7059–7066.

Mulert C, Jäger L, Schmitt R, Bussfeld P, Pogarell O, Möller H-J, *et al* (2004). Integration of fMRI and simultaneous EEG: towards a comprehensive understanding of localization and time-course of brain activity in target detection. *NeuroImage* **22**: 83–94.

Neo PS-H, McNaughton N (2011). Frontal theta power linked to neuroticism and avoidance. *Cogn Affect Behav Neurosci* **11**: 396–403.

Oakes TR, Pizzagalli DA, Hendrick AM, Horras KA, Larson CL, Abercrombie HC, *et al* (2004). Functional coupling of simultaneous electrical and metabolic activity in the human brain. *Hum Brain Mapp* **21**: 257–270.

Perrin F, Pernier J, Bertrand O, Echallier JF (1989). Spherical splines for scalp potential and current density mapping. *Electroencephalogr Clin Neurophysiol* **72**: 184–187.

Phillips JM, Vinck M, Everling S, Womelsdorf T (2013). A Long-Range Fronto-Parietal 5- to 10-Hz Network Predicts "Top-Down" Controlled Guidance in a Task-Switch Paradigm. *Cereb Cortex* bht050doi:10.1093/cercor/bht050.

Pivik RT, Broughton RJ, Coppola R, Davidson RJ, Fox N, Nuwer MR (1993). Guidelines for the recording and quantitative analysis of electroencephalographic activity in research contexts. *Psychophysiology* **30**: 547–558.

Pizzagalli DA, Iosifescu D, Hallett LA, Ratner KG, Fava M (2008). Reduced Hedonic Capacity in Major Depressive Disorder: Evidence from a Probabilistic Reward Task. *J Psychiatr Res* **43**: 76–87.

Pizzagalli DA, Oakes TR, Fox AS, Chung MK, Larson CL, Abercrombie HC, *et al* (2004). Functional but not structural subgenual prefrontal cortex abnormalities in melancholia. *Mol Psychiatry* **9**: 393–405.

Pizzagalli DA, Peccoralo LA, Davidson RJ, Cohen JD (2006). Resting anterior cingulate activity and abnormal responses to errors in subjects with elevated depressive symptoms: A 128-channel EEG study. *Hum Brain Mapp* **27**: 185–201.

Pizzagalli DA, Sherwood RJ, Henriques JB, Davidson RJ (2005). Frontal Brain Asymmetry and Reward Responsiveness A Source-Localization Study. *Psychol Sci* **16**: 805–813.

Schack B, Vath N, Petsche H, Geissler H-G, Möller E (2002). Phase-coupling of theta–gamma EEG rhythms during short-term memory processing. *Int J Psychophysiol* **44**: 143–163.

Tenke CE, Kayser J (2001). A convenient method for detecting electrolyte bridges in multichannel electroencephalogram and event-related potential recordings. *Clin Neurophysiol Off J Int Fed Clin Neurophysiol* **112**: 545–550.

Tsujimoto T, Shimazu H, Isomura Y, Sasaki K (2010). Theta Oscillations in Primate Prefrontal and Anterior Cingulate Cortices in Forewarned Reaction Time Tasks. *J Neurophysiol* **103**: 827–843.

Vitacco D, Brandeis D, Pascual-Marqui R, Martin E (2002). Correspondence of event-related potential tomography and functional magnetic resonance imaging during language processing. *Hum Brain Mapp* **17**: 4–12.

Wacker J, Dillon DG, Pizzagalli DA (2009). The role of the nucleus accumbens and rostral anterior cingulate cortex in anhedonia: Integration of resting EEG, fMRI, and volumetric techniques. *NeuroImage* **46**: 327–337.

Womelsdorf T, Johnston K, Vinck M, Everling S (2010). Theta-activity in anterior cingulate cortex predicts task rules and their adjustments following errors. *Proc Natl Acad Sci* **107**: 5248–5253.

Worrell GA, Lagerlund TD, Sharbrough FW, Brinkmann BH, Busacker NE, Cicora KM, *et al* (2000). Localization of the Epileptic Focus by Low-Resolution Electromagnetic Tomography in Patients with a Lesion Demonstrated by MRI. *Brain Topogr* **12**: 273–282.

Zumsteg D, Friedman A, Wennberg RA, Wieser HG (2005a). Source localization of mesial temporal interictal epileptiform discharges: Correlation with intracranial foramen ovale electrode recordings. *Clin Neurophysiol* **116**: 2810–2818.

Zumsteg D, Lozano AM, Wennberg RA (2006). Depth electrode recorded cerebral responses with deep brain stimulation of the anterior thalamus for epilepsy. *Clin Neurophysiol* **117**: 1602–1609.

Zumsteg D, Wennberg RA, Treyer V, Buck A, Wieser HG (2005b). H215O or 13NH3 PET and electromagnetic tomography (LORETA) during partial status epilepticus. *Neurology* **65**: 1657–1660.

Supplemental Table 1

Summary of Significant ROI-based Findings

Predictors	Dependent Variable	Frequency Band	Parameter Estimate (β)	*p*-value
sgACC	Neuroticism	Gamma	.31	.018*
rACC			ns	ns
dACC			ns	ns
OFC	Reward Learning	Gamma	.33	.004**
dlPFC (L)		Gamma	.34	.002**
dlPFC (R)			ns	ns
dACC			ns	ns
dlPFC (L)	Flanker Interference Effect (Accuracy)	Gamma	-.31	.009**
dlPFC (R)			ns	ns
dACC			ns	ns
rACC			ns	ns
dlPFC (L)	Flanker Interference Effect (RT)	Gamma	-.23	.045*
dlPFC (R)		Alpha2	.51	.012*
dACC		Theta, Alpha2	-.33, -.31	.019*, .020*
rACC			ns	ns

The table summarizes all significant findings from the primary ROI analyses predicting neuroticism, reward learning, Flanker interference effects on accuracy and reaction time (RT). As stated in the text, all effects control for site. sgACC = Subgenual anterior cingulate cortex (ACC; BA25); rACC = Rostral ACC (BA24/32); dACC = dorsal ACC (BA 24'/32'); OFC = Orbitofrontal cortex; dlPFC = Dorsolateral prefrontal cortex, left (L) and right (R) hemisphere.

*p<.05, **p<.01

Supplemental Figure S1. ***Regions-of-Interest (ROIs).*** Location and extent of (**A**) ACC subdivisions (BA25: 17 voxels; BA24: 12 voxels; BA32: 25 voxels; BA32': 20 voxels; BA24': 48 voxels: *BA25 = Subgenual ACC; BA24/32 = Rostral ACC; BA24'/32' = Dorsal ACC*), (**B**) OFC (BA11/13/47/12: 66 voxels), and (**C**) left and right dlPFC (lateral BA9: 73 voxels and BA46: 24 voxels) ROIs, as defined by the Structure-Probability Maps [Lancaster et al., 1997] and displayed on the LORETA template. Coordinates in mm (MNI space); origin at anterior commissure; (X) = left(–) to right(+); (Y) = posterior(–) to anterior(+); (Z) = inferior(–) to superior(+).